

## Effects of lattice deformation on magnetic properties of electron-doped $\text{La}_{0.8}\text{Hf}_{0.2}\text{MnO}_3$ thin films

Z. P. Wu, Y. C. Jiang, and J. Gao<sup>a)</sup>

*Department of Physics, The University of Hong Kong, Hong Kong*

(Presented 15 January 2013; received 3 November 2012; accepted 4 February 2013; published online 12 April 2013)

The lattice deformation effects on electric and magnetic properties of electron-doped  $\text{La}_{0.8}\text{Hf}_{0.2}\text{MnO}_3$  (LHMO) thin films have been systematically investigated. LHMO films with various thicknesses (15 nm, 40 nm, and 80 nm) were grown on (001)  $\text{SrTiO}_3$  and (001)  $\text{LaAlO}_3$  substrates, which induces in-plane tensile and compressive biaxial stress, respectively. The metal-insulator phase transition temperature ( $T_p$ ) and magnetoresistance (MR) effect show a strong dependence on film thickness.  $T_p$  increases with a decrease in thickness and is enhanced as the lattice strain rises, regardless of whether it is tensile or compressive. The maximum MR ratio is suppressed by reduction of the film thickness. These anomalous phenomena may be attributed to the competition between the strain induced modification of the Mn-O bond length and the  $e_g$  orbital stability. © 2013 AIP Publishing LLC. [<http://dx.doi.org/10.1063/1.4801336>]

Perovskite manganites have received enormous attention since the discovery of colossal magnetoresistance (CMR).<sup>1</sup> Early studies indicate that there are interactions between the local spin, charge, orbital and lattice degrees of freedom in manganites, resulting in rich physical phenomena.<sup>2,3</sup> At the same time, manganites are extremely sensitive to external disturbances, such as magnetic fields, electric fields, currents, mechanical strain, photo illumination, etc.<sup>4-7</sup> Among all variable factors, lattice mismatch induced biaxial strain plays an essential impact on the transport properties of manganites. The lattice deformation effect had been intensively investigated for decades. It is commonly believed that the Jahn Teller distortion is the main response for the modification of the transport properties.<sup>8,9</sup> The lattice strain could alter the radius of the ions inside the manganites, thus changes the size of  $\text{MnO}_6$  octahedral. A typical method to explore the lattice deformation effect is to adjust the thickness of epitaxial layers or deposit films on substrates with different lattice constants.<sup>6,10-12</sup>

So far, most of the efforts were devoted to hole-doped manganites with a double exchange (DE) interaction between  $\text{Mn}^{3+}/\text{Mn}^{4+}$ . Recently, tetravalent ions' substitution has stimulated much interest as a supplement for the hole-doping. Such electron-doped manganites may be of great potential for the development of all-manganites devices. However, the multivalent states in those tetravalent ions ( $\text{Ce}^{4+}$ ,  $\text{Te}^{4+}$ ,  $\text{Sb}^{4+}$ , and  $\text{Sn}^{4+}$ ) cause a debate on whether the intrinsic conduction mechanism is hole-doped or electron-doped DE effect.<sup>13,14</sup> Superior to other tetravalent elements, Hf has a sole tetravalent state, which makes it more reliable and relatively simple to study the electronic structures. From another aspect, with intermediate ionic radii [ $\text{Sn}^{4+}$  (0.081 nm) <  $\text{Hf}^{4+}$  (0.083 nm) <  $\text{Ce}^{4+}$  (0.097 nm) <  $\text{La}^{3+}$  (0.106 nm)],  $\text{Hf}^{4+}$  doped manganites are expected to show similar transport

properties as other electron-doped manganites.<sup>15,16</sup> In this paper, we report a systematic study on magnetic and electrical transport properties in the strained  $\text{La}_{0.8}\text{Hf}_{0.2}\text{MnO}_3$  (LHMO) thin films with varied thicknesses (15, 40, and 80 nm) on (001)  $\text{SrTiO}_3$  (STO) and (001)  $\text{LaAlO}_3$  (LAO) substrates, which introduce an in-plane biaxial tensile and compressive stress in the films, respectively.

LHMO film was fabricated on both STO and LAO single-crystal substrates by pulsed laser deposition (KrF excimer laser,  $\lambda = 248$  nm). The laser repetition rate and energy density were 1 Hz and  $3 \text{ J/cm}^2$ , respectively. The temperature of substrate was maintained at  $750^\circ\text{C}$  in a 0.5 mbar oxygen atmosphere. The thickness of the LHMO film is controlled by deposition time. To reduce the oxygen deficiency and improve the crystallinity, the as-grown film was *in situ* annealed at  $800^\circ\text{C}$  in an ambient atmosphere of high oxygen pressure (1 atm) for 1 h before cooling down to room temperature. Then, four silver contact pads with a diameter of  $200 \mu\text{m}$  were prepared on films by thermal evaporation. The transport properties were measured using a standard four-probe method.

The crystallinity and crystallographic orientation of the formed LHMO films were examined by x-ray diffraction (XRD). Figures 1(a) and 1(b) show the  $\theta$ - $2\theta$  spectrum of the LHMO films with 80 nm thickness deposited onto LAO and STO single crystal, respectively. Besides the (00 $l$ ) diffraction peaks from substrates and the LHMO films, no other peaks from the impurities or misorientation were visible, indicating a preferential  $c$ -axis growth of the LHMO layers. Figures 1(c) and 1(d) present the  $\theta$ - $2\theta$  patterns in a narrow range around the LHMO (002) reflection peaks with different thicknesses (80 nm, 40 nm, and 15 nm) on LAO and STO, respectively. The LHMO (002) reflection peaks on STO substrates were obtained by subtracting the  $K\alpha_2$  peaks of the STO (002) substrates. It can be observed that with decreasing thickness, both the LHMO (002) peaks become weaker. The position of the peaks shifts toward a lower degree on LAO in

<sup>a)</sup>Author to whom correspondence should be addressed. Electronic mail: [jugaoh@hku.hk](mailto:jugaoh@hku.hk)

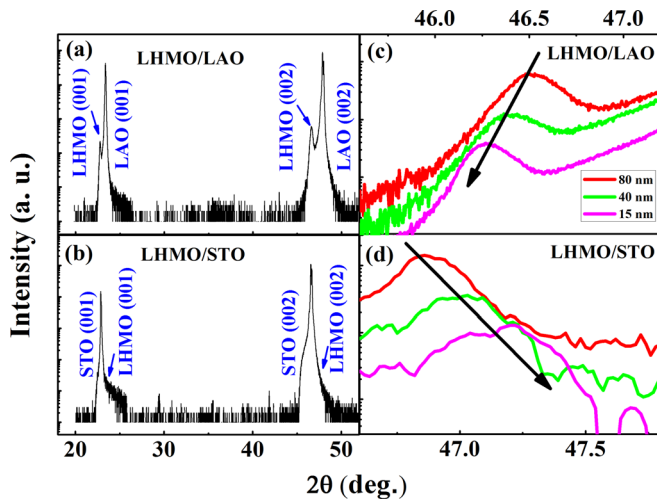


FIG. 1. (a) and (b) XRD  $\theta$ - $2\theta$  patterns of the LHMO 80 nm thick films deposited onto LAO and STO single crystal, respectively. (c) and (d)  $\theta$ - $2\theta$  spectrum in a narrow range of the LHMO films with different thickness values (80 nm, 40 nm, and 15 nm) grown on LAO and STO single crystal, respectively.

contrast to the shifts toward a higher degree on STO. The bulk LHMO ceramic is a distorted pseudocubic perovskite with a lattice parameter  $a = 3.882 \text{ \AA}$ . Our XRD diffraction results illustrate that the LHMO thin films grown on LAO ( $a = 3.798 \text{ \AA}$ ) substrates are under a biaxial compressive stress, which is induced by a  $-2.45\%$  lattice mismatch with the LAO substrate. On the other hand, the LHMO films grown on STO ( $a = 3.905 \text{ \AA}$ ) substrates are under a biaxial tensile stress with a  $+0.59\%$  lattice mismatch. From the position of LHMO (002) peaks in Figs. 1(c) and 1(d), the out-of-plane lattice parameter  $c$  and the strain  $\varepsilon_{zz}$  ( $\varepsilon_{zz} = c_{\text{film}} - c_{\text{bulk}}/c_{\text{bulk}}$ ) of the LHMO layers could be calculated. By using the Poisson relation  $\nu = 1/(1 - 2\varepsilon_{xx}/\varepsilon_{zz})$  with  $\nu = 0.37$ , the in-plane strain  $\varepsilon_{xx}$  could also be derived.<sup>17</sup> The calculated lattice parameters and the strain values are summarized in Table I.

Figure 2 plots the relationship between the thickness and the lattice parameters for LHMO grown on two types of substrates. With increasing thickness,  $c$  value expands and approaches the bulk value, whereas  $a$  value shrinks

TABLE I. Summary of the calculated values of lattice parameter  $c$ , out-of-plane strain  $\varepsilon_{zz}$ , lattice parameter  $a$ , in-plane strain  $\varepsilon_{xx}$ , metal-insulator transition temperature  $T_p$ , and MR peak values.

	Lattice parameter $c$ ( $\text{\AA}$ )	Out-of-plane strain (%)	Lattice parameter $a$ ( $\text{\AA}$ )	In-plane strain (%)	$T_p$	MR peak value (%)
LHMO/LAO (80 nm)	3.901	0.49	3.866	-0.42	251	86.7
LHMO/LAO (40 nm)	3.909	0.70	3.859	-0.60	255	72.8
LHMO/LAO (15 nm)	3.922	1.03	3.848	-0.88	295	63.7
LHMO/STO (80 nm)	3.873	-0.23	3.89	0.20	240	85.6
LHMO/STO (40 nm)	3.863	-0.49	3.898	0.42	242	77.6
LHMO/STO (15 nm)	3.849	-0.85	3.91	0.72	290	69.3

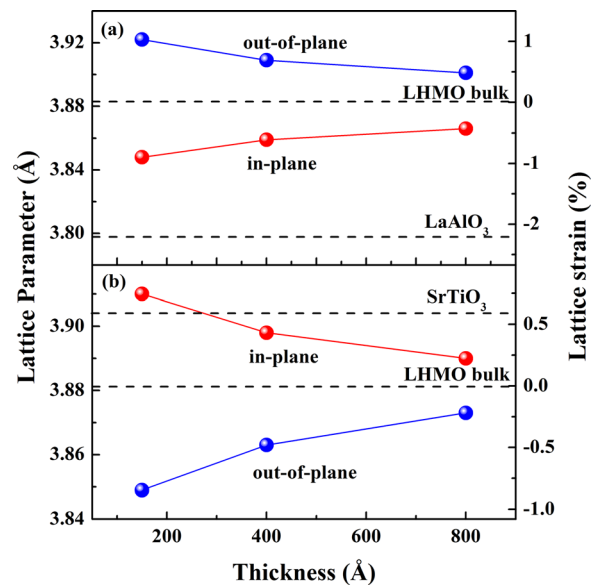


FIG. 2. Film thickness dependence of the out-of-plane and in-plane lattice parameters of epitaxial LHMO films grown on (a) LAO and (b) STO substrates. The bulk target and the substrates' lattice parameters are indicated by the horizontal dashed lines.

monotonically, indicating a relaxing of strain in the films. A larger  $c$  value and smaller  $a$  value will lead to a reduction in the Mn-O bond length  $d$  and an enhancement of the Mn-O-Mn bond angle. Therefore, the  $\text{MnO}_6$  octahedral will be distorted. Consequently, the DE interactions will compete with each other more strongly, with dependence on the structural distortion, giving rise to a magnetically disordered state. It can affect the magnetic and electrical transport properties of LHMO thin films dramatically. Values for LHMO films grown on LAO substrates are larger than the bulk one and decreases with increasing thickness.

Novel transport and magnetic properties were also found in LHMO thin films. Figures 3(a) and 3(b) present the temperature dependence of resistivity for LHMO thin films on two types of substrates under various magnetic fields ( $H = 0 \text{ T}$ ,  $1 \text{ T}$ ,  $3 \text{ T}$ , and  $5 \text{ T}$ ). In the absence of magnetic fields, a metal-insulator ( $MI$ ) transition occurs at a peak temperature  $T_p$  for all LHMO thin films. When a magnetic field is applied,

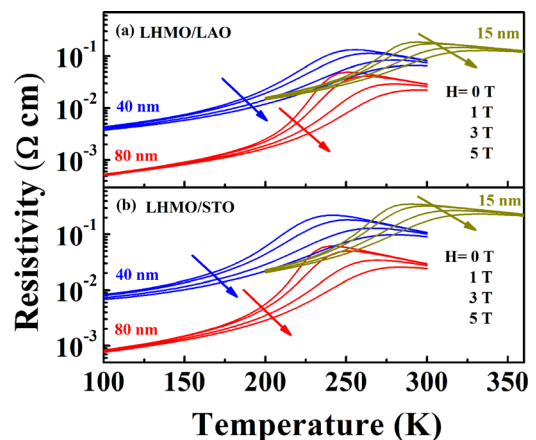


FIG. 3.  $R$ - $T$  curves for different thickness LHMO films grown on (a) LAO and (b) STO substrates under various magnetic fields (0 T, 1 T, 3 T, and 5 T).

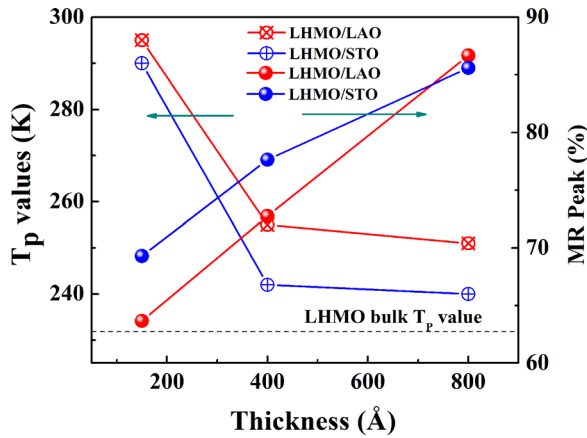


FIG. 4. Thickness dependence of the  $T_p$  and MR peak values for epitaxial LHM0 films grown on LAO and STO substrates.

the resistivity reduces in the whole temperature range and  $T_p$  moves toward higher temperatures continuously. Also, both the  $T_p$  and the resistivity of the films decrease with increasing film thickness. The decreasing resistivity is similar to other hole-doped manganites, which may attribute to a reduction of short range disorder or the defect in the films.<sup>18</sup> The  $T_p$  value and maximum value of magnetoresistance (defined as  $|MR| = |[R_H - R_0]/R_0 \times 100\%|$ ) are strongly dependent on film thickness. With decreasing thickness, the substrates' induced biaxial strain will increase. The enhanced biaxial strain may induce a distortion of  $MnO_6$  octahedron, which may reduce the double exchange interaction. Hence, the MR peak ratio will be suppressed. As shown in Figure 4, the maximum MR ratio is suppressed by the reduction of the film thickness. The bulk LHM0 ceramic exhibits a  $MI$  transition with a  $T_p$  of  $\sim 232$  K.<sup>19</sup> All formed films show raised  $T_p$  value with respect to the bulk. As seen in Table I, both in-plane strain  $\epsilon_{xx}$  and out-of-plane strain  $\epsilon_{zz}$  for LHM0 films grown on LAO substrates are larger.  $T_p$  value is greatly enhanced for 15 nm LHM0 films grown on either LAO or STO substrate. On STO substrates, when the thickness of LHM0 film reaches 80 nm,  $T_p$  value ( $\sim 240$  K) is comparable to that of bulk LHM0. However, although the  $T_p$  values in LHM0 films show strong dependence on film thickness, they do not show any correlation with strain states. Both tensile and compressive stresses shift the  $T_p$  values toward higher temperatures. This anomalous effect on  $T_p$  values differs from the common observations in doped manganites. This kind of unusual lattice deformation effect is not exclusively observed only in LHM0 films but also in other thin films such as

low doped  $La_{1-x}Ba_xMnO_3$  ( $x < 0.2$ ).<sup>3</sup> Several groups have reported an enhanced  $T_p$  value induced by a tensile strain.<sup>10,11</sup> A possible explanation is considering the  $e_g$  electron orbital stability modified by the induced strain. Due to the JT effect, the doublet  $e_g$  electron would split into two, i.e., the out-of-plane  $d_{3z^2-r^2}$  orbital and in-plane  $d_{x^2-y^2}$  orbital. The tensile strain would elongate the in-plane  $a$  value and thus stabilizes the  $d_{x^2-y^2}$  orbital. While the transfer intensity in the  $d_{x^2-y^2}$  orbital is larger than the  $d_{3z^2-r^2}$  orbital, the stabilization of the  $d_{x^2-y^2}$  orbital would raise electron hopping and DE interaction in LHM0 films, which lead to an increase of  $T_p$ . So, the competition between the strain induced modification of the Mn-O bond length and the  $e_g$  orbital stability might be responsible for the obtained enhanced  $T_p$  value. Other factors, such as oxygen deficiency and the stoichiometry of the formed thin films might also be taken into account to understand these anomalous phenomena.

Epitaxial LHM0 thin films with various thicknesses were deposited on LAO and STO substrates. Strong dependence of magnetic and electric transport properties on lattice deformation has been observed. As the film thickness decreases, both the tensile and compressive strain induced an enhancement of  $T_p$  and a suppression of the MR peak value. A competition between the strain induced Mn-O bond length and the  $e_g$  orbital stability was proposed to be responsible for the anomalous strain effect.

This work has been supported by a grant of the Research Grant Council of Hong Kong (Project No. HKU 702112 P) and the Seed Funding of the University of Hong Kong.

- <sup>1</sup>S. Jin *et al.*, *Science* **264**, 413 (1994).
- <sup>2</sup>A. P. Ramirez *et al.*, *Phys. Rev. Lett.* **76**, 3188 (1996).
- <sup>3</sup>J. Zhang *et al.*, *Phys. Rev. B* **64**, 184404 (2001).
- <sup>4</sup>T. Wu *et al.*, *Phys. Rev. Lett.* **86**, 5998 (2001).
- <sup>5</sup>A. Asamitsu *et al.*, *Nature* **388**, 50 (1997).
- <sup>6</sup>R. A. Rao *et al.*, *Appl. Phys. Lett.* **73**, 3294 (1998).
- <sup>7</sup>F. X. Hu and J. Gao, *Appl. Phys. Lett.* **88**, 132502 (2006).
- <sup>8</sup>W. Eerenstein *et al.*, *Nature Mater.* **6**, 348 (2007).
- <sup>9</sup>R. K. Zheng *et al.*, *Appl. Phys. Lett.* **90**, 152904 (2007).
- <sup>10</sup>M. Kanai, H. Tanaka, and T. Kawai, *Phys. Rev. B* **70**, 125109 (2004).
- <sup>11</sup>T. Kanki *et al.*, *Phys. Rev. B* **71**, 012403 (2005).
- <sup>12</sup>C. Adamo *et al.*, *Appl. Phys. Lett.* **95**, 112504 (2009).
- <sup>13</sup>J. Gao, S. Y. Dai, and T. K. Li, *Phys. Rev. B* **67**, 153403 (2003).
- <sup>14</sup>G. T. Tan *et al.*, *Phys. Rev. B* **68**, 014426 (2003).
- <sup>15</sup>J. R. Sun *et al.*, *Phys. Rev. B* **67**, 144414 (2003).
- <sup>16</sup>J. H. Hao, J. Gao, and D. P. Yu, *Appl. Phys. Lett.* **87**, 131908 (2005).
- <sup>17</sup>J. F. Nye, *Physical Properties of Crystals* (Oxford University Press, New York, 1985), p. 143.
- <sup>18</sup>M. Bibes *et al.*, *Phys. Rev. B* **66**, 134416 (2002).
- <sup>19</sup>E. J. Guo *et al.*, *J. Appl. Phys.* **110**, 113914 (2011).